Organic & Biomolecular Chemistry

Accepted Manuscript

ROYAL SOCIETY OF CHEMISTRY

www.rsc.org/obc

Journal Name

ARTICLE TYPE

Cite this: DOI: 10.1039/xxxxxxxxxx

Dithiafulvenyl-substituted phenylacetylene derivatives: Synthesis and structure–property–reactivity relationships†

Yunfei Wang and Yuming Zhao*

Received Date
Accepted Date

DOI: 10.1039/xxxxxxxxxx

www.rsc.org/journalname

A series of regioisomers for dithiafulvenyl-substituted phenylacetylene derivatives was synthesized and characterized to show structure-dependent electronic properties and different reactivity in their oxidized states.

The application of π–conjugated materials has achieved a tremendous advancement in the cutting-edge fields such as molecular electronics, chemo-/bio-sensors, light-emitting devices, and organic photovoltaics.[1–3] From the chemistry perspective, continued efforts to explore π-molecular building blocks with novel properties and functions are still imperative and highly needed. For decades, tetrathiafulvalene (TTF)—the first organic conductor—has played an indispensable and central role in the area of molecular electronics.[4] In modern TTF chemistry, a myriad of π–extended TTF analogues (*i.e.*, exTTFs) have been synthesized and many of them were found to show intriguing redox, optoelectronic, and supramolecular properties.[5–8] Among numerous types of exTTFs, the so-called tetrathiafulvalene vinylogues (TTFVs)[9,10] have been actively pursued by us[11] and others[12–14] over the past few years. A particularly appealing aspect of TTFVs, especially aryl-substituted TTFVs, is its redox-controllable conformational switching behavior.[11,14,15] Built upon aryl-TTFVs, various functional molecular systems have been prepared and reported recently, including stimuli-responsive conjugated polymers,[16,17] fluorescent molecular tweezers,[18,19] redox-active ligands,[12] shape-persistent macrocycles,[20,21] and molecular rotors.[22] Of note is our previous study on certain alkynylated TTFV systems derived from a phenylacetylene-substituted dithiafulvene (DTF) precursor **1a** (Fig. 1).[20,21] Herein the inclusion of alkynyl group in this DTF compound greatly enhances its synthetic versatility by enabling diverse efficient C–C bond forming reactions to take place on both the DTF unit and the alkynyl group.[18–21,23] Our previous study on **1a** naturally led us to pondering on its two other regioisomers, **1b** and **1c** (Fig. 1). As building blocks, acetylenic DTF isomers **1a–c** would give rise to π–conjugated materials with different structures and properties as a result of their different molecular shapes and π–conjugation patterns. In this context, it is of fundamental importance to conduct comparative studies on the properties and reactivity of **1a–c** as well as the π–extended systems derived from them.

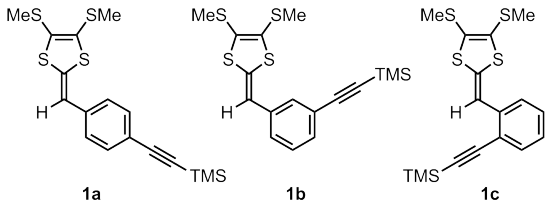

Fig. 1 Structures of acetylenic DTFs **1a–c**.

The synthesis of DTFs **1a–c** was executed through a phosphite-promoted olefination method,[24,25] using trimethylsilylethynyl–substituted benzaldehydes **2a–c** and thione **3** as the starting materials (Scheme 1). Experimentally, the three olefination reactions went completion in 3 hours at 105 °C, giving the desired products **1a–c** with similar yields (*ca*. 75–79%). Compounds **1a–c** were then subjected to an oxidative coupling[26] in CH_2Cl_2 at room temperature using iodine as oxidant (Scheme 1). The reactions yielded acetylenic diphenyl-TTFVs **3a–c** in very good yields. Note that in our previous work, certain *ortho*-substituents (Br and Me) would retard the deprotonation step in the oxidative dimerization mechanism, leading to the formation of a unique bis-spiro structure other than the typical TTFV product.[27,28] This scenario however did not happen in the oxidative dimerization of *ortho*-alkynyl DTF **1c**, because the alkynyl group is linear-shaped and much less bulkier.

Besides the oxidative dimerization reactions, the acetylenic

Department of Chemistry, Memorial University, St. John's, NL A1B 3X7, Canada. Fax: 1 709 864 3702; Tel: 1 709 864 8747; E-mail: yuming@mun.ca

† Electronic Supplementary Information (ESI) available: Detailed synthetic procedures and characterization data for new compounds. See DOI: 10.1039/b000000x/

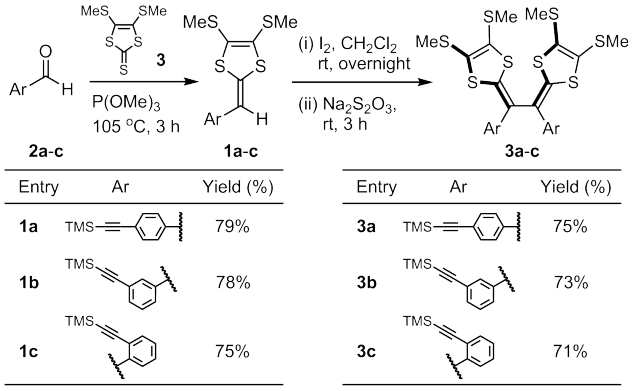

Scheme 1 Synthesis of acetylenic DTFs **1a–c** and related TTFV derivatives **3a–c**.

DTF synthons could also be synthetically elaborated to attain π–extension through alkynyl coupling reactions. Scheme 2 outlines the Hay coupling reactions[29] of desilylated **1a–c**. The synthesis began with protiodesilylation with K_2CO_3 to first generate free terminal alkyne intermediates, which after a brief workup were immediately subjected to alkynyl homocoupling catalyzed by CuI/TMEDA, affording bis(DTF)–endcapped conjugated butadiynes **4a–c** in satisfactory yields. Diynes **4a** and **4b** are yellow coloured solids, whereas **4c** shows an intense orange color, suggesting that it has very different electronic absorption properties than the other two isomers (*vide infra*).

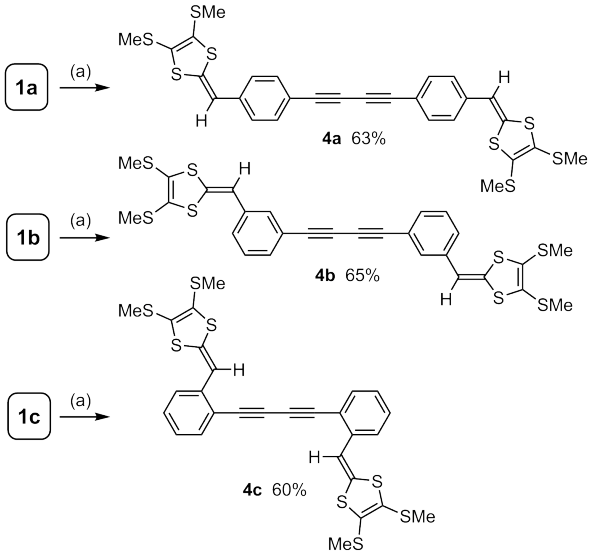

Scheme 2 Synthesis of bis(DTF)-endcapped butadiynes **4a–c** via Hay coupling. (a) (i) K_2CO_3, THF/MeOH, 30 min, (ii) CuI, TMEDA, air, CH_2Cl_2, rt, 5 h.

The electronic absorption properties of acetylenic DTFs and their related π–derivatives were studied by UV–Vis spectroscopy. As can been from Fig. 2, the three DTF isomers **1a–c** show $\pi \rightarrow \pi^*$ transition bands with similar molar absorptivity. The maximum absorption wavelengths (λ_{max}) shift in a trend of **1a** (384 nm) > **1b** (376 nm) > **1c** (357 nm), giving a qualitative comparison for the degree of π–delocalisation among the three isomers. The observation of **1c** showing the lowest λ_{max} value in the three isomers can be reasonably correlated with its *ortho*-substitution structure which engenders the most significant steric interactions between the alkynyl group and the DTF moiety to attenuate the π–conjugation.

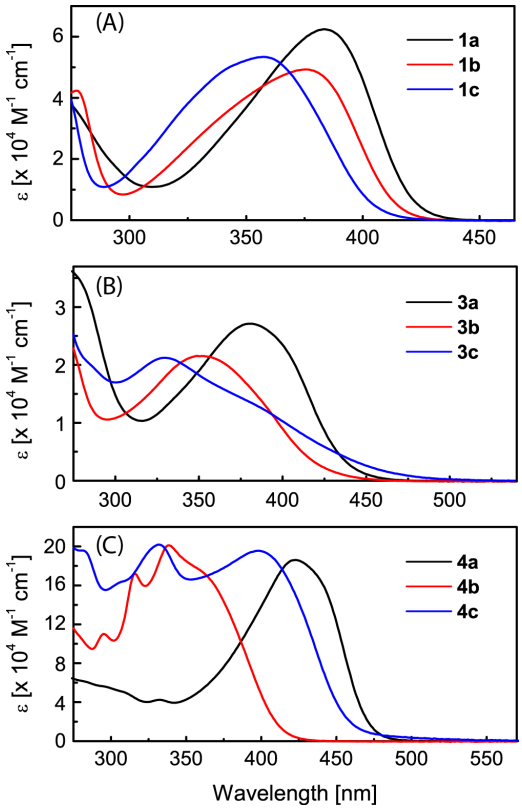

Fig. 2 UV-Vis absorption spectra of compounds **1a–c**, **3a–c**, and **4a–c** measured in CH_2Cl_2 at room temperature.

The $\pi \rightarrow \pi^*$ transition bands of TTFV isomers **3a–c** show the same trend of λ_{max} shift (*i.e.*, *para* > *meta* > *ortho*) as that in **1a–c**, but the extent of variation is much greater (Fig. 2B). For *para*-isomer **3a** the λ_{max} value is observed at 380 nm, which is nearly identical to that of its DTF precursor **1a** and indicates that the central TTFV moiety in **3a** does not contribute to increasing π–delocalisation due to its twisted *cis*-like conformation.[11,15,30] Compared with **3a**, the absorption peak of *meta*-isomer **3b** shows a significant blueshift to 350 nm, which is suggestive that the π–electron delocalisation in **3b** is more disrupted than **3a**. The absorption spectrum of *ortho*-isomer **3c** differs pronouncedly from its other two isomers, wherein the λ_{max} value at 329 nm is considerably blueshifted. In addition, the spectrum of **3c** features a broad absorption slope in the range of *ca*. 350 to 500 nm. Worth noting is that such a spectral profile bears great resemblance to that of a bis(1-naphthyl)-TTFV compound[31] we reported previously. Given that the central TTFV moiety of the bis(1-naphthyl)-TTFV has been confirmed to assume a completely planar *trans* conformation by X-ray analysis,[31] the molecular shape of **3c** is thus deemed as adopting a similar *trans* motif. Further evidence for this conformational argument can be elicited from the cyclic voltammetric analysis (*vide infra*).

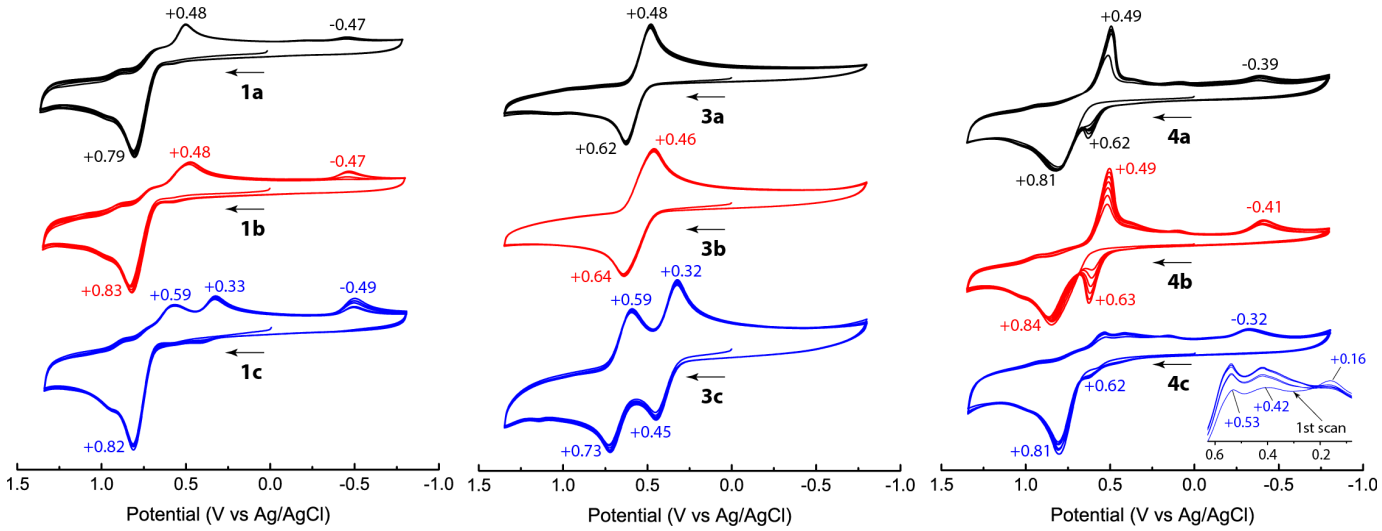

Fig. 3 Cyclic voltammograms of compounds **1a–c**, **3a–c**, and **4a–c** measured in CH_2Cl_2 at room temperature. Experimental conditions: supporting electrolyte: Bu_4NBF_4 (0.1 M), working electrode: glassy carbon, counter electrode: Pt wire, reference electrode: Ag/AgCl (3 M NaCl), scan rate: 200 mV s^{-1}.

The UV-Vis spectral profiles of bis(DTF)-endcapped butadiynes **4a–c** varied significantly from one to another (Fig. 2C). The spectrum of diyne **4a** shows a monotonous absorption peak centred at 423 nm, with absorptivity in the range of 270–350 nm being very low. The spectral envelope of **4b** is substantially blueshifted relative to **4a**, showing three well-resolved bands at 339, 316, and 295 nm and a shoulder peak at 361 nm, respectively. The spectrum of **4c** gives two intense $\pi \rightarrow \pi^*$ bands at 398 and 332 nm. Overall, the λ_{max} values of the bis(DTF)–butadiyne isomers **4a–c** follow an order of *para* > *ortho* > *meta*, which is different from those of DTFs **1a–c** and TTFVs **3a–c**. An empirical rationalization for such spectroscopic behavior can be made based on the π-delocalisation degree argument; that is, the DTF–phenylene–diyne skeletons of compounds **4a** and **4c** are in linear π–conjugation, whereas that of compound **4b** is cross-conjugated due to its *meta*-substitution pattern.

The redox properties of compounds **1a–c**, **3a–c**, and **4a–c** were characterized by cyclic voltammetry (CV), and the detailed voltammograms are shown in Fig. 3. When scanned in the positive direction, DTFs **1a–c** all show a similar anodic peak at *ca.* +0.8 V which can be assigned to the formation of [$DTF^{\cdot+}$] radical cation via a single-electron oxidation step.[15,32] In the reverse scan, a cathodic peak at +0.48 V is seen in the voltammograms of *para*- and *meta*-isomers **1a** and **1c**. Compared with the voltammograms of TTFVs **3a** and **3b**, the origin of this current peak can be assigned to the two-electron reduction of the [$TTFV^{2+}$] dication formed on the working electrode surface through electrochemical oxidative dimerization. For *ortho*-isomer **1c**, the reverse CV scan reveals two cathodic peaks at +0.59 and +0.33 V respectively in the positive potential window. These two peaks are ascribed to the stepwise single-electron transfers occurring on the [$TTFV^{2+}$] product, which is evidenced by the nearly identical reduction features observed in the voltammogram of *ortho*-alkynyl TTFV **3c**. In the negative potential window, all the voltammograms of **1a–c** show a noticeable cathodic peak around –0.47 V. The intensity of this peak shows dependence on scan rate; that is, at relatively slow rate this peak just diminishes. It is therefore reasoned that this particular anodic peak is associated with some intermediary species formed electrochemically which would readily diffuse away from the working electrode surface.

The voltammograms of TTFVs **3a** and **3b** both show a similar reversible redox wave pair, which can be unambiguously assigned to the simultaneous two-electron redox processes on the diphenyl-substituted TTFV moiety which normally would take a twisted *cis*-like conformation.[11,15,30] Significantly different are the patterns in the voltammogram of *ortho*-isomer **3c**, in which the redox processes of TTFV undergo two distinct single-electron steps. Such CV behaviour, according to the previous studies by Yamashita[30] and us,[31] alludes to a scenario that the TTFV moiety in **3c** prefers a planar *trans* conformation. The *ortho*-alkynyl groups in **3c** are believed to play a key role in directing the central TTFV conformation.

Likewise, the CV analysis of bis(DTF)-endcapped butadiynes **4a-c** also discloses notable substitution effects on their redox properties. The voltammograms of *para*- and *meta*-isomers **4a** and **4b** show the typical DTF oxidation peak at *ca.* +0.8 V along with a steadily growing redox wave pair due to the formation of TTFV during multicycle CV scans. The CV results confirm that **4a** and **4b** can readily undergo electrochemical polymerization through the oxidative DTF coupling.[15,20,33,34] Interestingly, such reactivity appears to be disfavoured in the case of *ortho*-isomer **4c**, for there is no observation of the characteristic TTFV redox wave pair in its voltammogram. Worth noting is that the CV profile of **4c** exhibits an irreversible pattern with a few weak cathodic current peaks discernible in the reverse scans (see the inset in Fig. 3), suggesting that the oxidation of **4c** is followed by some swift chemical transformations to form redox-inactive species.

To gain a deeper insight into the redox reactivity, bis(DTF)–diynes **4a–c** were subjected to chemical oxidation using iodine as oxidant. In line with the electrochemical analysis, diynes **4a**

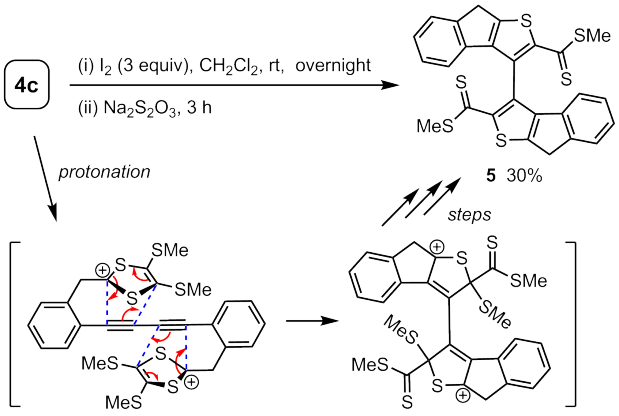

Scheme 3 Formation of compound **5** via an intramolecular cycloaddition pathway.

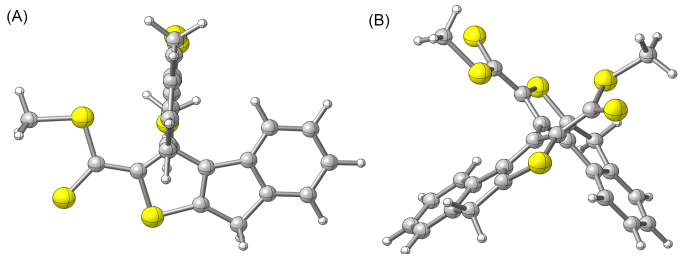

Fig. 4 Optimized structure of compound **5** at the B3LYP/6-31G(d) level. (A) Front view, (B) side view.

and **4b** under oxidative conditions were efficiently converted into corresponding TTFV–diyne oligomers, which were validated by MALDI-TOF MS analysis (see ESI). The same oxidative treatment of *ortho*-isomer **4c**, to our great surprise, ended up with the formation of a major product **5** (Scheme 3) along with a number of intractable byproducts. MS analysis confirmed that the byproducts were not TTFV–diyne oligomeric products. Compound **5** is a red coloured solid and electron-accepting in nature. The cyclic voltammogram of **5** clearly shows a reversible redox wave pair in the negative potential region (E_{pa} = –1.08 V, E_{pc} = –1.25 V), without any obvious redox peaks in the positive window (see ESI). The mechanism for the formation of **5** is a rather complex one and awaits further investigations to be fully disclosed. At this juncture, a two-fold intramolecular cycloaddition[35,36] pathway is tentatively proposed (Scheme 3) to account for the formation of the fused aromatic moieties in **5**. Density functional theory (DFT) calculations suggest that the two fused aromatic units in **5** are nearly perpendicular to one another (see Fig. 4) in orientation. The biaryl-type structure and the presence of two thioester groups in the scaffold of **5** point to a potential in ligand design and stereoselective catalysis.[37]

In summary, a series of structurally isomeric acetylenic DTFs and their π–extended derivatives have been systematically synthesized and characterized. Our studies show that the different substitution patterns in these compounds exert important effects on their electronic and redox properties. Worth highlighting is that *ortho*-alkynyl substituted TTFV derivatives and conjugated butadiyne systems behave in a dramatically different way in terms of electronic absorption and redox reactivity compared with their *para*- and *meta*-isomers. The structure-property-reactivity relationships established herein offer a useful guidance to the ongoing research of DTF and alkyne based conjugated materials.

References

1 *Functional Organic Materials: Syntheses, Strategies and Applications*, ed. T. J. J. Müller and U. H. F. Bunz, Wiley-VCH, Weinheim, Germany, 2006.
2 G. Inzelt, *Conducting Polymers: A New Era in Electrochemistry*, Sprin, Berlin, 2nd edn, 2012.
3 A. Facchetti, *Chem. Mater.*, 2011, **23**, 733–758.
4 *TTF Chemistry: Fundamentals and Applications of Tetrathiafulvalene*, ed. J.-i. Yamada and T. Sugimoto, Springer, Berlin, 2004.
5 D. Canevet, M. Salle, G. Zhang, D. Zhang and D. Zhu, *Chem. Commun.*, 2009, 2245–2269.
6 M. Bendikov, F. Wudl and D. F. Perepichka, *Chem. Rev.*, 2004, **104**, 4891–4946.
7 J. L. Segura and N. Martín, *Angew. Chem. Int. Ed.*, 2001, **40**, 1372—1409.
8 M. R. Bryce, *J. Mater. Chem.*, 1995, **5**, 1481–1496.
9 A. J. Moore and M. R. Bryce, *Tetrahedron Lett.*, 1992, **33**, 1373–1376.
10 L. Yu and D. Zhu, *Chem. Commun.*, 1997, 787–788.
11 Y. Zhao, G. Chen, K. Mulla, I. Mahmud, S. Liang, P. Dongare, D. W. Thompson, L. N. Dawe and S. Bouzan, *Pure Appl. Chem.*, 2012, **84**, 1005–1025.
12 E. Gontier, N. Bellec, P. Brignou, A. Gohier, M. Guerro, T. Roisnel and D. Lorcy, *Org. Lett.*, 2010, **12**, 2386–2389.
13 J. Massue, N. Bellec, M. Guerro, J. F. Bergamini, P. Hapiot and D. Lorcy, *J. Org. Chem.*, 2007, **72**, 4655–4662.
14 M. Guerro, R. Carlier, K. Boubekeur, D. Lorcy and P. Hapiot, *J. Am. Chem. Soc.*, 2003, **125**, 3159–3167.
15 N. Bellec, K. Boubekeur, R. Carlier, P. Hapiot, D. Lorcy and A. Tallec, *J. Phys. Chem. A*, 2000, **104**, 10994–10994.
16 S. Liang, Y. Zhao and A. Adronov, *J. Am. Chem. Soc.*, 2014, **136**, 970–977.
17 S. Liang, G. Chen, J. Peddle and Y. Zhao, *Chem. Commun.*, 2012, **48**, 3100–3102.
18 K. Mulla, H. Shaik, D. W. Thompson and Y. Zhao, *Org. Lett.*, 2013, **15**, 4532–4535.
19 K. Mulla, P. Dongare, D. W. Thompson and Y. M. Zhao, *Org. Biomol. Chem.*, 2012, **10**, 2542–2544.
20 G. Chen, I. Mahmud, L. N. Dawe, L. M. Daniels and Y. Zhao, *J. Org. Chem.*, 2011, **76**, 2701–2715.
21 G. Chen, I. Mahmud, L. N. Dawe and Y. Zhao, *Org. Lett.*, 2012, **12**, 704–707.
22 G. Chen and Y. Zhao, *Org. Lett.*, 2014, **16**, 668–671.
23 K. Mulla and Y. Zhao, *Tetrahedron Lett.*, 2014, **55**, 382–386.
24 S. S. Schou, C. R. Parker, K. Lincke, K. Jennum, J. Vibenholt, A. Kadziola and M. B. Nielsen, *Synlett*, 2013, **24**, 231–235.
25 C. A. Christensen, A. S. Batsanov and M. R. Bryce, *J. Org. Chem.*, 2007, **27**, 1301–1308.
26 P. Hapiot, D. Lorcy, A. Tallec, R. Carlier and A. Robert, *J. Phys. Chem.*, 1996, **100**, 14823–14827.
27 S. Bouzan, L. N. Dawe and Y. Zhao, *Tetrahedron Lett.*, 2013, **54**, 4666–4669.
28 K. Woolridge, L. C. Goncalves, S. Bouzan, G. Chen and Y. Zhao, *Tetrahedron Lett.*, 2014, **55**, 6362–6366.
29 A. S. Hay, *J. Org. Chem.*, 1962, **27**, 3320–3321.
30 Y. Yamashita, M. Tomura, M. B. Zaman and K. Imaeda, *Chem. Commun.*, 1998, 1657–1658.
31 S. Bouzan, G. Chen, K. Mulla, L. N. Dawe and Y. Zhao, *Org. Biomol. Chem.*, 2012, **10**, 7673–7676.
32 J. Massue, J. Ghilane, N. Bellec, D. Lorcy and P. Hapiot, *Electrochem. Commun.*, 2007, **9**, 677 – 682.
33 S. Inagi, K. Naka, D. Iida and Y. Chujo, *Polym. J.*, 2006, **38**, 1146–1151.
34 K. Naka, S. Inagi and Y. Chujo, *J. Polym. Sci. Part A: Polym. Chem.*, 2005, **43**, 1099–0518.
35 G. Meazza, G. Zanardi, G. Guglielmetti and P. Piccardi, *J. Fluor. Chem.*, 1997, **82**, 175–180.
36 R. Mancuso and B. Gabriele, *Molecules*, 2014, **19**, 15687–15719.
37 A. Shockravi, A. Javadi and E. Abouzari-Lotf, *RSC Adv.*, 2013, **3**, 6717–6746.